Pure Appl. Geophys. 174 (2017), 1061–1070

DOI 10.1007/s00024-016-1430-9

Pure and Applied Geophysics

3D Density Modeling with Gravity and Muon-Radiographic Observations in Showa-Shinzan Lava Dome, Usu, Japan

Ryuichi Nishiyama,[1,2] Seigo Miyamoto,[1] Shuhei Okubo,[1] Hiromitsu Oshima,[3] and Tokumitsu Maekawa[3]

Abstract—We performed three-dimensional density modeling of Showa-Shinzan lava dome, Usu, Japan, by joint inversion of the gravity anomaly and recently obtained muon radiography data. Our multilayer emulsion muon detector significantly reduces the background noise in our measurements of the muon flux through the dome. The high-quality muon data enables us to more accurately reconstruct the density structure of the lava dome compared with our own previous work. We find that the lava dome consists of a cylindrical column of massive lava with a diameter of 300 m, and that there is no evidence of magma intrusion in the shallow part of the plateau, located east of the dome.

1. Introduction

Muon radiography is a recently developed method that can be used to probe the internal density profile of geophysical structures (Okubo and Tanaka 2012). The method is based on measurements of the absorption of cosmic-ray induced muons passing through matter. Since the energy spectrum of muons has been well studied and the muon penetration length as a function of energy has been confirmed (Groom et al. 2001), the attenuation of the muon flux can be used to derive the column density of an object along muon trajectories. Mt. Showa-Shinzan (Fig. 1), which is a target volcano of the present study, has been surveyed with muon radiography by Tanaka et al. (2007). The muon detector used in the work is a four-layer stack of emulsion films, special photographic films for experimental particle physics. The detector was exposed to cosmic rays for three months at 500 m south of the dome summit. The muon absorption rates obtained from the detector allowed to reveal a two-dimensional density profile of the volcano. With the publication of this work, muon radiography has gained attention and has been used for a variety of applications such as monitoring of volcanoes (Lesparre et al. 2012; Ambrosino et al. 2015), seismic faults (Tanaka et al. 2011), caves (Oláh et al. 2012) and etc.

Gravity exploration is also used to determine the density of geophysical structures. Therefore, the combination of gravity anomalies and muon radiography should give a stronger constraint on the density profile than muon radiography alone. In our previous paper (Nishiyama et al. 2014a), we proposed joint inversion for determining the three-dimensional density profiles of volcanoes, and demonstrated the feasibility using the muon radiography data of Tanaka et al. (2007) and our own gravity data for Mt. Showa-Shinzan. The resulting 3D density model revealed the shape of the lava inside the mountain (see Figs. 2b, 3b). However, there are two issues with the model: (i) an unrealistically high density ($\sim 2800\,\mathrm{kg/m^3}$) was derived at the summit region of the dome, which is inconsistent with the dacite (silicic) lava that comprises the dome, (ii) the model suggests that high-density lava was deflected 300 m to the south at around 300 m above sea level (asl), but such a deflection is not supported by geological or geophysical observations.

We believe the problems with the previous density model likely arose from the poor accuracy of the density estimation based on muon radiography. In fact, recent studies have shown that interference from background particles ($\lesssim$1 GeV) can lead to systematic uncertainty in

[1] Earthquake Research Institute, The University of Tokyo, 1-1-1, Yayoi, Bunkyo-ku, Tokyo 113-0032, Japan. E-mail: ryuichi.nishiyama@lhep.unibe.ch

[2] Laboratory for High-Energy Physics, Albert Einstein Center for Fundamental Physics, University of Bern, Sidlerstrasse 5, 3012 Bern, Switzerland.

[3] Usu Volcano Observatory, Graduate School of Science, Hokkaido University, 142, Tatsuka, Sobetsu-cho, Usu-gun, Hokkaido 052-0106, Japan.

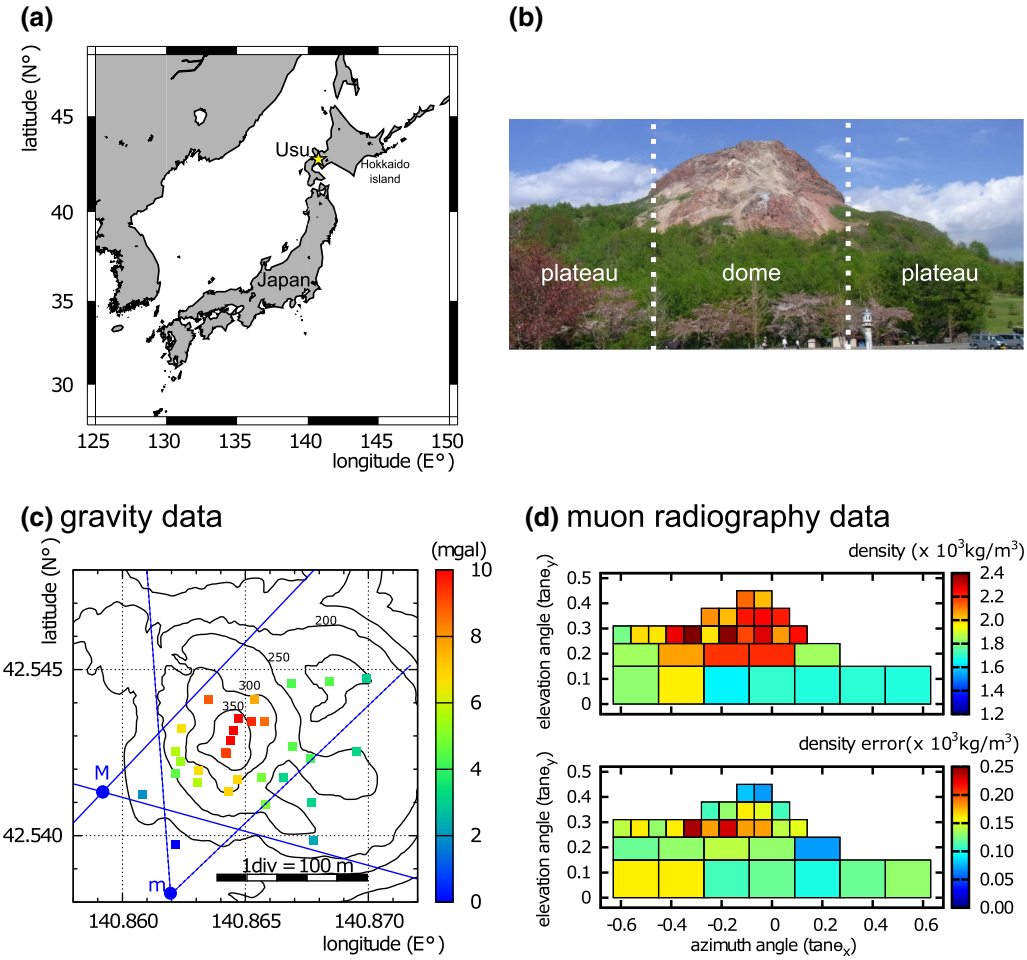

Figure 1

a Location of the Usu volcanic region. **b** Mt. Showa-Shinzan seen from the muon detector site. The mountain is characterized by a lava dome and the plateau surrounding it. **c** Free-air gravity anomaly values relative to the reference station. "M" shows the position of the new muon detector and the two *blue beams* crossing at M show the viewing range of the muon radiography observation. "m" indicates the detector position of Tanaka et al. (2007). **d** Average density determined from muon radiography (*upper*) and associated error (*lower*)

density estimation by muon detectors with low-energy thresholds (Nishiyama et al. 2014b, 2016; Ambrosino et al. 2015). Therefore, we obtained a new set of observations at Showa-Shinzan, with the emulsion detector configured to reduce the background particles. The aim of the present paper is to update the 3D density model using the new muon radiography data and to discuss the mechanism of lava dome formation.

2. Method

Several studies have considered the joint inversion of gravity anomaly and muon radiography data (e.g. Davis and Oldenburg 2012; Nishiyama et al. 2014a; Jourde et al. 2015). The basic idea lying is that one should find a density model which agrees with the observed gravity and muon data simultaneously. Davis and Oldenburg (2012) and Nishiyama et al. (2014a) have formulated this problem as a linear inverse problem. When the volume of interest is discretized into n voxels with density $\rho_j (j = 1, 2, \ldots, n)$, the gravity and muon data can be written as linear combinations of the unknown density values. Specifically, the vertical component of the gravity anomaly at the ith gravity station is then expressed as

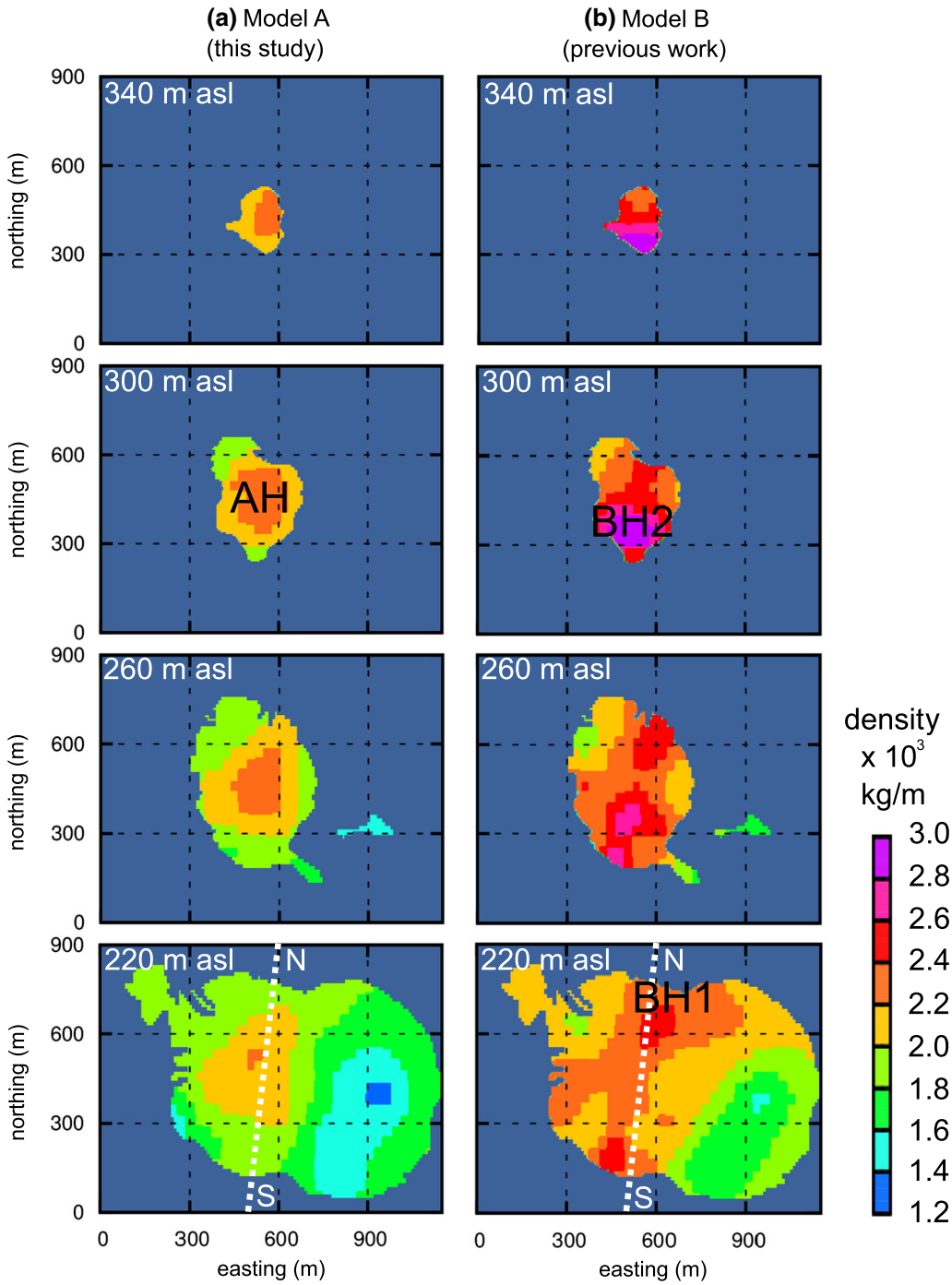

Figure 2
Horizontal cross-sectional views of the density model at altitudes of 340, 300, 260 and 220 m asl (**a** this study, **b** previous work by Nishiyama et al. (2014a)). A *vertical* cross-sectional view along the line S-N is given in Fig. 3

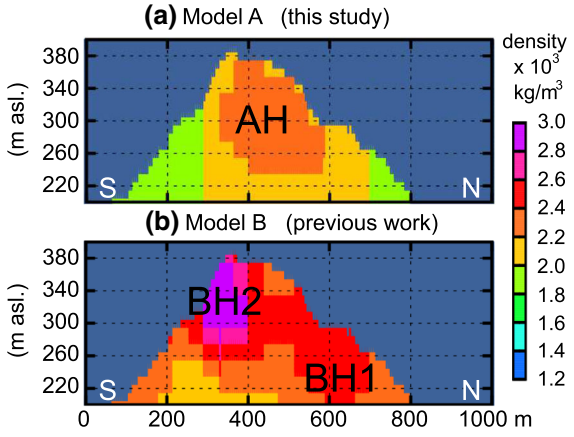

Figure 3
Vertical cross sectional-views of the density model along the line S-N shown in Fig. 2 (**a** this study, **b** previous work by Nishiyama et al. (2014a))

$$\Delta g_i = \Delta g(x_i, y_i, z_i) = \sum_j^n G_{ij}\rho_j, \tag{1}$$

where G_{ij} is the vertical gravity contribution of the jth voxel to the ith gravity station for unit density. The column-density (sometimes referred to as the density-length or opacity in the literature) derived from muon radiography, is written as

$$X_i = \sum_j^n L_{ij}\rho_j, \tag{2}$$

where L_{ij} is the length of the ith muon trajectory crossing the jth voxel. These two equations can be simplified to

$$\mathbf{d} = \mathbf{A}\boldsymbol{\rho}, \tag{3}$$

where $\mathbf{d}$ and $\mathbf{A}$ are the integrated data vector and integrated design matrix:

$$\mathbf{d} = \begin{pmatrix} \mathbf{X} \\ \mathbf{\Delta g} \end{pmatrix}, \ \mathbf{A} = \begin{pmatrix} \mathbf{L} \\ \mathbf{G} \end{pmatrix}. \tag{4}$$

Nishiyama et al. (2014a) have treated this inverse problem through a Bayesian approach (Tarantola and Nercessian 1984). Given the observed data $\mathbf{d}_{\text{obs}}$, the solution of Eq. (3) is expressed as

$$\boldsymbol{\rho}' = \boldsymbol{\rho}_0 + (\mathbf{A}^{\mathrm{T}}\mathbf{C}_{\mathbf{d}}^{-1}\mathbf{A} + \mathbf{C}_{\rho}^{-1})^{-1}\mathbf{A}^{\mathrm{T}}\mathbf{C}_{\mathbf{d}}{}^{-1}(\mathbf{d}_{\text{obs}} - \mathbf{A}\boldsymbol{\rho}_0) \tag{5}$$

with covariance matrix written as

$$\mathbf{C}'_{\rho} = (\mathbf{A}^{\mathrm{T}}\mathbf{C}_{\mathbf{d}}^{-1}\mathbf{A} + \mathbf{C}_{\rho}^{-1})^{-1}, \tag{6}$$

where ρ_0 is an initial guess density, and $\mathbf{C}_{\rho}$ and $\mathbf{C}_{\mathbf{d}}$ are covariance matrices for the initial guess and the data. To cope with the illposedness of the problem, a smoothing constraint is introduced on model parameters through an exponential covariance function:

$$C_{\rho}(p, q) = \sigma_{\rho}^2 \exp(-d(p, q)/l), \tag{7}$$

where σ_{ρ} is the magnitude of the uncertainty, l is the correlation length and $d(p, q)$ is the distance between the pth and qth voxels.

The advantage of the above-mentioned method is that one can obtain a solution with enough precisions by simple matrix calculation. Furthermore, a lot of effort is paid to develop a more comprehensive inversion scheme. For instance, Jourde et al. (2015) have developed an advanced treatment for the muon flux data which varies non-linearly with density and they have demonstrated the advantages of the joint inversion through numerical simulation.

3. Data

3.1. Geological Setting

Mt. Showa-Shinzan is a parasitic cone of Usu Volcano, located at the southern rim of Toya Caldera, Hokkaido, Japan (Fig. 1a). Major historical eruptions have been recorded in 1663, 1768, 1822, 1853, 1910, 1943, 1977 and 2000. Mt. Showa-Shinzan was formed in the end of the event of 1943. The present topography of the mountain is characterized by the dome and the plateau (Fig. 1b). The diameter of the dome is $\sim$300 m and the altitude of the peak is 398 m. The gravity data were taken on the dome and the plateau. The new muon detector was placed so that the field of view encloses the dome and the plateau. Details are given in the following subsections.

3.2. Gravity Data

The gravity data used in this analysis was collected by the authors in 2011 (see Nishiyama et al. 2014a). A total of 30 gravity stations were used,

giving a coverage of approximately 600 m × 600 m. The position of each gravity station is measured by GPS interferometry, and the horizontal and vertical positioning is accurate to within 2–3 and 10 cm, respectively. The free-air gravity anomaly is used for data set of the inversion (Fig. 1c). Although Bouguer anomaly is often used for geoexploration, the reason for choice of the free-air anomaly is that it contains the whole gravity effect from the sea level to the surface, which has to be modeled in the inversion.

The calculation of the terrain response and the matrix element (G_{ij}) is done using a digital elevation model (DEM) published by the Geospatial Information Authority of Japan. The elevation data are given every 0.2" for both longitude and latitude. The accuracy of the elevation is $\Delta h = 3.2$ m, because the difference between the digital elevation and the position of our 30 gravity stations from GPS measurement is confirmed to follow a Gaussian distribution with a standard deviation of 3.2 m. The dominant error in the inversion, therefore, arises from the inaccuracy of the DEM on which the gravity calculation relies. We estimate the magnitude of the error to be $2\pi\rho\mathcal{G}\Delta h \sim 300\ \mu$gal (gal $= 10^{-2}$ ms^{-2} and $\mathcal{G}$ is the gravitational constant) by calculating the gravity from an infinite plate with an uniform density of $\rho = 2100$ kg/m^3.

3.3. Muon-Radiography Data

We performed a new muon radiography observation with a different setup from the previous measurement by Tanaka et al. (2007). In the last measurement, a stack of four emulsion films were employed as a muon detector. However, recent studies show that the observation with such a thin detector would be severely contaminated by background noise arising from low-energy charged particles. For instance, Ambrosino et al. (2015) have suffered from an overwhelming background noise because their detector did not have enough absorber. Nishiyama et al. (2016) have identified that the origins of those background particles are low-energy ($\lesssim$1 GeV) protons, electrons and muons which hit the detector independently of high-energy muons after passing through the target mountain.

To reduce the background contamination, we used an improved multilayer detector with thin lead plates inserted between emulsion films. Specifically, the detector consists of 20 sheets of emulsion films and nine 1-mm-thick lead plates. The charged particles with $E \sim 1$ GeV are scattered typically 5 mrad after passing through the lead plate. Since the resolution of track angle recognition with microscopes is better than 5 mrad, the trajectories of the low-energy background particles can be identified and rejected for further analysis. The emulsion film used in this exposure was OPERA type (Nakamura et al. 2006), which was developed by a collaboration between Nagoya University and FUJIFILM Corporation for a neutrino oscillation experiment called OPERA (Oscillation Project with Emulsion-tRacking Apparatus). The OPERA film consists of a 200-μm-thick plastic base and 50-μm-thick sensitive layers of emulsion poured on both sides of the base.

The new detector was installed 500 m west to the dome summit at an altitude of 189 m. The coverage volume of the muon paths is almost same from the previous study (Fig. 1c). The effective area of the detector is $S = 104$ cm^2 and the observation time is $T = 1.45 \times 10^7$ sec (168 days, November 2011–May 2012). The exposure condition ($ST = 1.5 \times 10^5$ m^2 sec) is also in the same order of magnitude with the previous measurement ($\sim 4.5 \times 10^5$ m^2 sec). After exposure, the emulsion films were chemically developed, and the tracks recorded on them were read using the ESS (European Scanning System; Arrabito et al. 2006). Reconstruction of the tracks was performed using the FEDRA (Framework for Emulsion Data Reconstruction and Analysis; Tioukov et al. 2006) system. The reconstructed tracks were then grouped into thirty rectangular bins and the muon flux was estimated for each bin after efficiency correction. The muon flux was then converted into the average density along the radial direction from the detector (Fig. 1d). We account for the statistic fluctuation of the incoming muon flux in the density error.

4. Result

We choose a priori parameters as follows: initial density $\rho_0 = 1900$ kg/m^3, initial density error $\sigma_\rho =$

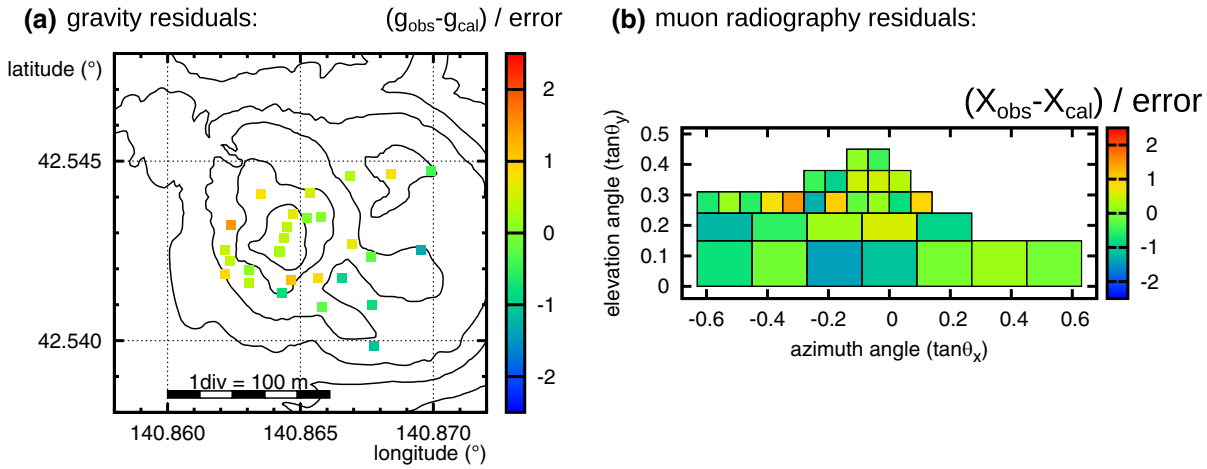

Figure 4
Residuals between the observed and calculated data for **a** gravity data and **b** muon radiography data, normalized with each observation error (**a** 300 μgal, **b** density estimation error shown in Fig. 1d multiplied by the length of a muon path)

300 kg/m^3 and correlation length $l = 100$ m. We determined the initial density and corresponding error from the mean and standard deviation of the density values in the thirty bins of the muon radiography image. Once these parameters were obtained, the observed data were inverted for the density model using Eq. (5). The resulting density model is shown in Fig. 2a (horizontal cross sections). The vertical cross section is shown in Fig. 3a and three dimensional representation of the model is shown in Fig. 6.

The model explains the observed gravity and muon data well (Fig. 4). For quantitative discussion, we define chi-square values as differences between observed and calculated data:

$$\chi^2_{\mathrm{muon}} \equiv (\mathbf{X}_{\mathrm{obs}} - \mathbf{L}\boldsymbol{\rho}')^{\mathrm{T}}\mathbf{C}^{-1}_{\mathrm{d,muon}}(\mathbf{X}_{\mathrm{obs}} - \mathbf{L}\boldsymbol{\rho}') \quad (8)$$

and

$$\chi^2_{\mathrm{grav}} \equiv (\Delta\mathbf{g}_{\mathrm{obs}} - \mathbf{G}\boldsymbol{\rho}')^{\mathrm{T}}\mathbf{C}^{-1}_{\mathrm{d,grav}}(\Delta\mathbf{g}_{\mathrm{obs}} - \mathbf{G}\boldsymbol{\rho}'), \quad (9)$$

where $\mathbf{C}_{\mathrm{d,muon}}$ and $\mathbf{C}_{\mathrm{d,grav}}$ are the covariance matrices for muon radiography and gravity observations. The result is $\chi^2_{\mathrm{muon}} = 21.3$ (number of data is 30) and $\chi^2_{\mathrm{grav}} = 14.0$ (number of data is 30) (Fig. 4). Since these are small and roughly equal to the degrees of freedom of the data space, we may assume that our model provides a good fit to the data. The estimation error is given by the diagonal elements of the posterior covariance matrix $\mathbf{C}'_{\boldsymbol{\rho}}$ (Fig. 5a). The error is about 200 kg/m^3 for most locations, and is improved to approximately 150 kg/m^3 near the summit because the gravity stations are densely distributed there. In the eastern area of the uplifted plateau, where the density of gravity stations is low, the density error is no less than 300 kg/m^3, which is almost the same as the original error.

We evaluated the spatial resolution of the inversion using a checkerboard reconstruction test. We defined a density function $\boldsymbol{\rho}_{\mathrm{syn}}$, which consisted of alternating high-density ($\rho_{\mathrm{high}} = 2200$ kg/m^3) and low-density ($\rho_{\mathrm{low}} = 1600$ kg/m^3) voxels with horizontal dimensions of 200 m $\times$ 200 m and vertical dimension of 100 m (Fig. 5b). This 3D checkerboard density pattern, superimposed on the topography of the mountain enabled us to synthesize the data $\mathbf{d}_{\mathrm{syn}}$, i.e., the column density ($\mathbf{X}$) for the thirty muon trajectories and the gravity anomaly values ($\Delta\mathbf{g}$) for the thirty gravity stations. We generated Gaussian random noise from the data covariance matrix ($\mathbf{C}_{\mathrm{d}}$) and added it to $\mathbf{d}_{\mathrm{syn}}$. The reconstructed density pattern is shown in Fig. 5b. Although the checkerboard pattern is not fully reproduced due to the correlation assumption, the position and the amplitude of anomaly are reproduced. Thus, the resolution of this inversion in the horizontal and vertical directions is better than 200 and 100 m, respectively. The resolution is comparable to that of the previous work

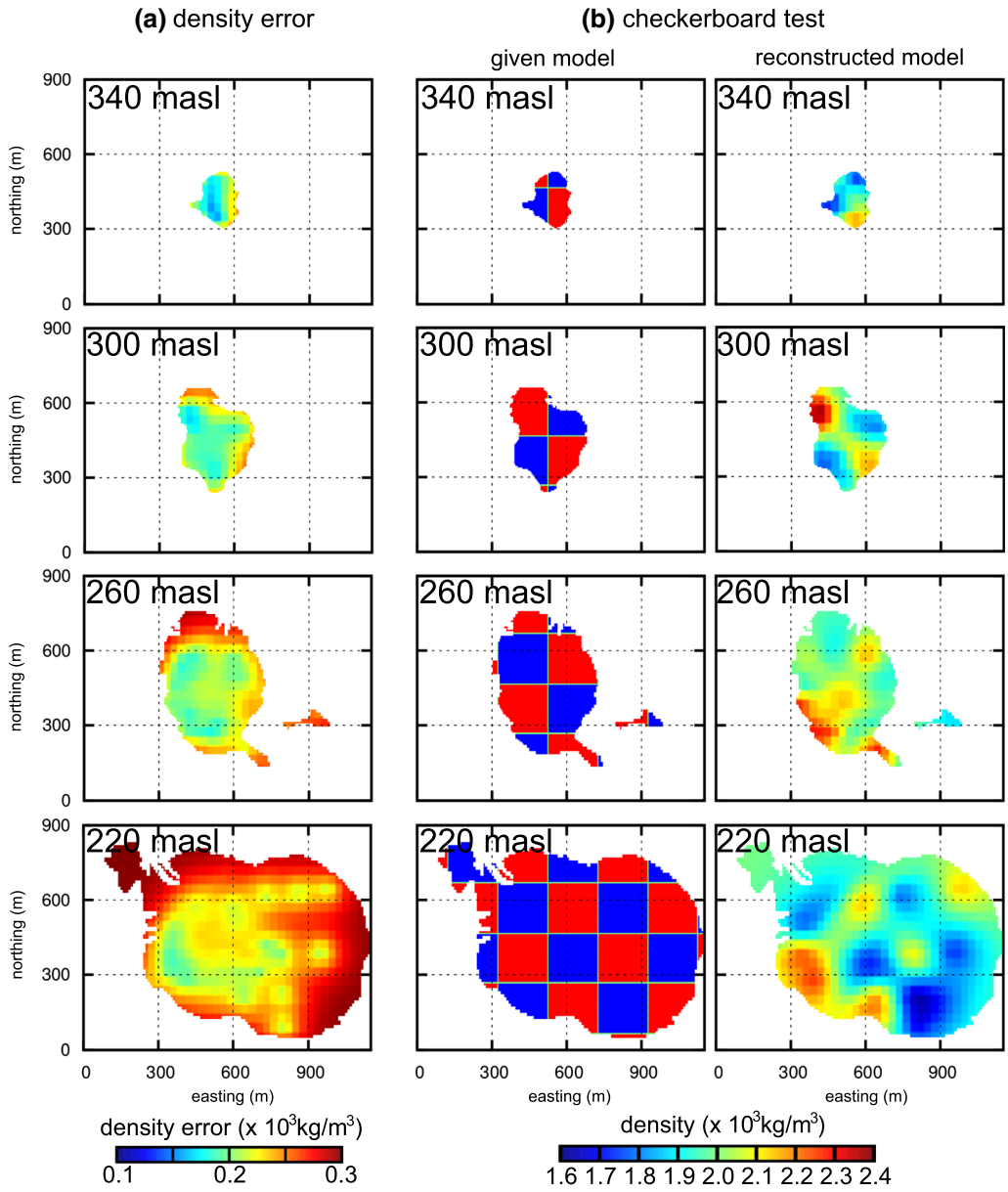

Figure 5
a Error associated with the 3D density model of the present study. **b** Checkerboard pattern used as input for the resolution test (*left*) and the reconstructed density model (*right*)

(Nishiyama et al. 2014a), in spite of the different position of the muon detectors (Fig. 6).

5. Discussion

The 3D density model derived from the present work (Model A, Fig. 2a) is much more geophysically reasonable than the previous 3D model (Model B, Fig. 2b) in several respects. First, the density values of the dome region (AH: 2.0–2.4 $\times$ 10^3 kg/m^3) is consistent to 2.32 $\times$ 10^3 kg/m^3, the bulk density of dacite lava on Mt. Showa-Shinzan (Nemoto et al. 1957). It also agrees with the terrain density of the mountain body of Usu (2.2 $\times$ 10^3, kg/m^3) estimated from Bouguer anomaly analysis by Komazawa et al.

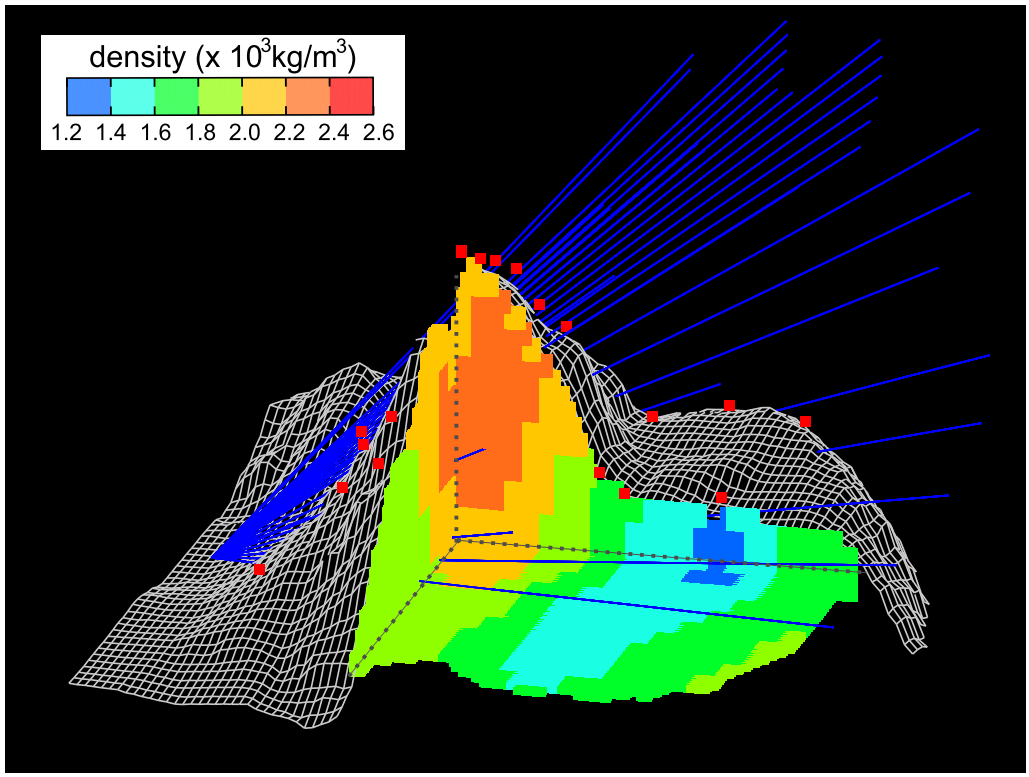

Figure 6
Three-dimensional representation of the density model developed in this study. The positions of the gravity stations are shown with *red solid squares*, and the muon trajectories are drawn with *blue lines*

(2010). On the other hand, the previous model exhibited unacceptably higher density of 2.6–3.0 $\times$ 10^3 kg/m^3 in the region BH2. Considering that the lava constituting the dome is hypersthene dacite (Oba et al. 1983), these density values are too high to be justified. The better values of rock density in the present study are due to the improved accuracy of muon radiography accomplished by our new detector, because the coverage and exposure condition are almost same with the previous muon observation. Second, Model A reveals a high-density column (AH) with a diameter of 300 m penetrating the center of the dome from deep within the interior, while the previous study requires high density blocks to be separated in two regions, BH1 (2.4–2.6 $\times$ 10^3 kg/m^3 at 220 m asl) and BH2 (2.6–3.0 $\times$ 10^3 kg/m^3 at 340 m asl). The latter model leads to a strange and unnatural interpretation that the lava suddenly migrates horizontally by around 300 m at a height of 300 m asl.

Since after the eruption and the morphographic development of the dome were recorded by several researchers (Minakami et al. 1951; Mimatsu 1962), various ideas have been proposed for the mechanism of lava dome formation. Nemoto et al. (1957) concluded from several observations that the lava block extends to below sea level and its diameter increases with depth, where the visible portion is only "the tip of the iceberg". On the other hand, Nishida and Miyajima (1984) claimed that the diameter of the lava block remains constant with depth, based on geomagnetic observations. A recent magnetotelluric observation (Goto and Johmori 2014) suggests the existence of a subspherical dacite intrusion ($\sim$400 m across). The results of the present study (Model A) are in agreement with Nishida and Miyajima (1984) and Goto and Johmori (2014). Our model contradicts with the hypothesis that the diameter of the lava block increases with depth as proposed by Nemoto et al. (1957). Our results would give clues also on

how the plateau was formed. Several prior works have proposed the existence of lava intrusion in the eastern plateau to explain the huge deformation (Nakamura and Mori 1949; Nemoto et al. 1957; Nishida and Miyajima 1984). However, the present study indicates an absence of massive lava at a shallow depth since there is no corresponding region of high density in our model. This conclusion agrees with the recently compiled gravity surveys (Komazawa et al. 2010; Geological Survey of Japan 2013) and recent resistivity model (Goto and Johmori 2014). Goto and Johmori (2014) suggests that the plateau was formed by the uplift of the ground and lateral migration of pre-existing rocks and sediment from the dome region. The present study supports the notion from the viewpoints of density.

The density model of the present study is limited above 200 m asl, because the muon radiography has no sensitivity below the altitude of the detector. However, the resolution of the deeper part would be improved if muon data from several directions are available, as numerically demonstrated by Jourde et al. (2015). In near future, such a multi-directional observation will be possible by emulsion film detectors, since they are light and they do not require power supply for operation.

6. Conclusion

The 3D density model of the Mt. Showa-Shinzan lava dome was updated using a joint inversion analysis of the gravity anomaly and muon radiography data obtained using a multilayer emulsion detector. The results indicate that the lava dome has a cylindrical shape (300 m in diameter) of massive lava block ($2.0–2.4 \times 10^3\,\mathrm{kg/m^3}$), and that there is no intruding body at a shallow depth of the eastern plateau. The results of this investigation clearly demonstrates the usefulness of the multilayer emulsion detector for muon radiography.

Acknowledgements

We thank Prof. Mitsuhiro Nakamura and his colleagues at the F-lab, Nagoya University for technical assistance with the emulsion films. We thank Dr. Cristiano Bozza and Dr. Valeri Tioukov for their enormous help with the emulsion analysis. We thank Mr. Saburo Mimatsu for giving permission to conduct the gravity survey on Mt. Showa-Shinzan. Beautification Escort Staff at Shikotsu-Toya National Park kindly offered us the site for muon radiography observations. We thank two anonymous reviewers for beneficial comments to improve the manuscript. This work was supported in part by JSPS KAKENHI Grant Number 23244092. One of the authors (R. N.) was supported by JSPS Fellowship (DC2, 25-9317) during this project.

References

Ambrosino, F., Anastasio, A., Bross, A., Béné, S., Boivin, P., Bonechi, L., et al. (2015). Joint measurement of the atmospheric muon flux through the Puy de Dôme volcano with plastic scintillators and Resistive Plate Chambers detectors. *Journal of Geophysical Research Solid Earth*, *120*(11), 7290–7307. (2015JB011969).OA.

Arrabito, L., Barbuto, E., Bozza, C., Buontempo, S., Consiglio, L., Coppola, D., et al. (2006). Hardware performance of a scanning system for high speed analysis of nuclear emulsions. *Nuclear Instruments and Methods A*, *568*, 578–587.

Davis, K., & Oldenburg, D. W. (2012). Joint 3D inversion of muon tomography and gravity data to recover density. *ASEG Extended Abstracts*, *1*, 1–4.

Geological Survey of Japan. (2013). *Gravity Database of Japan DVD edition, digital geoscience map P-2*. Tsukuba: Geological Survey of Japan, AIST.

Goto, Y., & Johmori, A. (2014). Resitivity structure of the Showa-Shinzan dome at Usu volcano, Hokkaido, Japan. *Bulletin of the Volcanological Society of Japan*, *59*, 1–11.

Groom, D. E., Mokhov, N. V., & Striganov, S. I. (2001). Muon stopping power and range tables 10 MeV–100 TeV. *Atomic Data and Nuclear Data Tables*, *78*, 183–356.

Jourde, K., Gibert, D., & Marteau, J. (2015). Improvement of density models of geological structures by fusion of gravity data and cosmic muon radiographies. *Geoscientific Instrumentation Methods and Data Systems*, *4*, 177–188.

Komazawa, M., Okuma, S., Matsushima, N., & Satoh, H. (2010). Explanation note of gravity anomaly map–geophysical maps of Usu Volcano, digital geoscience Map P-7(CD). AIST: Geological Survey of Japan.

Lesparre, N., Gibert, D., Marteau, J., Komorowski, J., Nicollin, F., & Coutant, O. (2012). Density muon radiography of La soufriére of Guadeloupe volcano: Comparison with geological, electrical resistivity and gravity data. *Geophysical Journal International*, *190*(2), 1008–1019.

Mimatsu, M., (1962). Diary of the growth of Showa-Shinzan: Mimatsu Masao Memorial Museum.

Minakami, T., Ishikawa, T., & Yagi, K. (1951). The 1944 eruption of volcano Usu in Hokkaido, Japan. *Bulletin Volcanologique*, *11*, 45–157.

Nakamura, S., & Mori, T. (1949). On the mechanism of the formation of the Showa new mountain of Usu volcano. *Science Reports of the Tohoku Imperial University Series*, *5*(1), 45–49.

Nakamura, T., Ariga, A., Ban, T., Fukuda, T., Fukuda, T., Fujioka, T., et al. (2006). The OPERA film: New nuclear emulsion for large-scale, high-precision experiments. *Nuclear Instruments and Methods A*, *556*, 80–86.

Nemoto, T., Hayakawa, M., Takahashi, K., & Oana, S. (1957). Report on geological, geophysical and geochemical studies of Usu volcano (Showa-Shinzan): Rep. *Geological Survey of Japan*, *170*, 1–149.

Nishida, Y., & Miyajima, E. (1984). Subsurface structure of Usu volcano, Japan as revealed by detailed magnetic survey. *Journal of Volcanology and Geothermal Research*, *22*, 271–285.

Nishiyama, R., Tanaka, Y., Okubo, S., Oshima, H., Tanaka, H. K. M., & Maekawa, T. (2014a). Integrated processing of muon radiography and gravity anomaly data toward the realization of high-resolution 3-D density structural analysis of volcanoes: Case study of Showa-Shinzan Lava Dome, Usu, Japan. *Journal of Geophysical Research Solid Earth*, *119*, 699–710.

Nishiyama, R., Miyamoto, S., & Naganawa, N. (2014b). Experimental study of source of background noise in muon radiography using emulsion film detectors. *Geoscientific Instrumentation Methods and Data Systems*, *3*, 29–39.

Nishiyama, R., Taketa, A., Miyamoto, S., & Kasahara, K. (2016). Monte Carlo simulation for background study of geophysical inspection with cosmic-ray muons. *Geophysical Journal International*, *206*, 1039–1050.

Oba, Y., Katsui, Y., Kurasawa, H., Ikeda, Y., & Uda, T. (1983). Petrology of historic rhyolite and dacite from Usu volcano, North Japan. *Journal of the Faculty of Science Hokkaido University Series IV*, *20*, 274–290.

Okubo, S., & Tanaka, H. K. M. (2012). Imaging the density profile of a volcano interior with cosmic-ray muon radiography combined with classical gravimetry. *Measurement Science and Technology*, *23*, 16.

Oláh, L., Barnaföldi, G. G., Hamar, G., Melegh, H. G., & Varga, D. (2012). CCC-based muon telescope for examination of natural caves. *Geoscientific Instrumentation Methods and Data Systems*, *1*, 229–234.

Tanaka, H. K. M., Nakano, T., Takahashi, S., Yoshida, J., Ohshima, H., Maekawa, T., et al. (2007). Imaging the conduit size of the dome with cosmic-ray muons: The structure beneath Showa-Shinzan lava dome, Japan. *Geophysical Research Letters*, *34*(22), L22311.

Tanaka, H. K. M., Miyajima, H., Kusagaya, T., Taketa, A., Uchida, T., & Tanaka, M. (2011). Cosmic muon imaging of hidden seismic fault zones: Rainwater premeation into the mechanical fractured zones in Itoigawa-Shizuoka Tectonic Line, Japan. *Earth and Planetary Science Letters*, *306*(3), 156–162.

Tarantola, A., & Nercessian, A. (1984). Three-dimensional inversion without blocks. *Geophysical Journal of the Royal Astronomical Society*, *76*, 299–306.

Tioukov, V., Kreslo, I., Petukhov, Y., & Sirri, G. (2006). The FEDRA: Framework for emulsion data reconstruction and analysis in the opera experiment. *Nuclear Instruments and Methods A*, *559*, 103–105.

(Received February 1, 2016, revised November 13, 2016, accepted November 15, 2016, Published online November 24, 2016)